◆❖ Scientific
❖◆ Research

Synthesis and Characterisations of TiO₂ Coated Multiwalled Carbon Nanotubes/Graphene/Polyaniline Nanocomposite for Supercapacitor Applications

Debasis Ghosh[1], Soumen Giri[1], Swinderjeetsingh Kalra[2], Chapal Kumar Das[1*]

[1]Materials Science Centre, Indian Institute of Technology Kharagpur, Kharagpur, India
[2]Department of Chemistry, Dayanand Anglo-Vedic (D.A.-V.) College, Kanpur, India
Email: [*]chapal12@yahoo.co.in

ABSTRACT

Nowadays with ever increasing demand of energy, developing of alternative power sources is an important issue all over the world. In this respect we have prepared nanocomposites based on metal oxide (titanium oxide) coated multi-walled carbon nanotubes (MWCNTs)/polyaniline (PANI) with graphene and without graphene and studied their electrochemical performance. The formation of the polymer in the nanocomposites was confirmed by the Fourier Transform Infrared Spectroscopy (FTIR) study. The morphological characterisations were carried out by the Field Emission Scanning Electron Microscopy (FESEM) and Transmission Electron Microscopy (TEM). To characterize the prepared nanocomposites electrode, a cyclic voltammetry test for measuring specific capacitance, and an impedance test were conducted. The highest value of specific capacitance obtained for the TiO₂ coated MWCNTs/PANI nanocomposite was 443.57 F/g at 2 mV/s scan rate. Upon addition of graphene nanosheet to the TiO₂ coated MWCNTs in a weight ratio of (9:1) the specific capacitance value increased to 666.3 F/g at the same scan rate, also resulting in an increase in energy density and power density.

Keywords: Supercapacitors; Polyaniline; Nanocomposites; Graphene Nanosheet

1. Introduction

Supercapacitors, also known as electrochemical capacitors or ultracapacitors are of interest in terms of their high energy density and high power density as well as pollution free long term energy supply source. Conventional capacitor has the property of high power density but suffers from low energy density, whereas, conventional battery has got the property of high energy density but low power density. Supercapacitors form a bridge between the two by combining the high energy density and high power delivery status. Supercapacitors store energy either by the formation of electrical double layer at the electrode electrolyte interface, typically known as Electric Double Layer Capacitor (EDLC) or by the pseudocapacitance mechanism or by both. The charge storage mechanism in EDLC is non-faradaic *i.e.* no electron transfer reaction occurs and the process is directly electrostatic [1]. EDLC increases the rate of response but suffers from comparatively less amount of charge storage. In case of redox supercapacitor, the active species undergoes fast and reversible oxidation and reduction. The pseudocapacitance, which arises due to electron transfer redox process, causes typically 10 times greater charge storage comparable to that of EDLC. Typically, designing of a supercapacitor requires three essential components, the electrodes, the electrolyte and the separator. The supercapacitor electrode plays the role of charge storage/delivery and determines energy density and power density [2]. For the supercapacitor electrode materials, carbon materials, conducting polymer and metal oxides are mostly used [3]. Carbon materials such as activated carbon, nano porous carbon materials were used previously but now these are replaced mostly by CNT and graphene. The charge storage mechanism in pristine CNT is due to electrical double layer formation and it has got very good absorption characteristic due to the accessible mesopores formed by the entangled individual CNTs [4]. However the specific capacitance of pristine CNT is low and due to their bundle structure, their effective surface area decreases. This results in their restricted use in many devices. Graphene is an outstanding material for supercapacitor electrode owing to its very high surface area (2675 m²/g), high thermal conductivity, extreme electrical conductivity and very high mechanical strength. Use of metal oxide as electrode materials such

---

[*]Corresponding author.

as RuO_2, MnO_2, SnO_2, NiO [5-8] have been studied in detail. The combination of CNT or graphene with the metal oxide also has been investigated in the recent years. A. L. M. Reddy and S Ramaprabhu obtained specific capacitance of 138 and 93 F/g for RuO_2/MWNT and SnO_2/MWNT nanocomposite electrodes respectively [9]. For the graphene metal oxide nanocomposites, Cheng *et al.* obtained a specific capacitance of 328 F/g for MnO_2/graphene at 1mA charging current [10], whereas, Wang et al reported high specific capacitance of 855 F/g for $Ni(OH)_2$/graphene nanocomposites at 5mV/s scan rate and 367 F/g for RuO_2/graphene at 2 mV/s scan rate [11]. Conducting polymers such as, polypyrrole, polyaniline (PANI), polythiophene are used as another part of electrode material. Among the various conducting polymers, PANI has been studied extensively due to its low cost, easy synthesis procedure, redox reversibility as well as good environmental stability and moderated electrical conductivity [1,12]. Graphene or CNT combines with the conducting polymer and stores energy by the electronic and ionic charge separation as well as by the faradaic charge transfer across the electrode electrolyte interface [1,13-16]. CNT and graphene have free surface pi-electrons. The surface pi-electrons can interact strongly with PANI through the quinoid ring and thereby facilitate the functionalization of CNT and graphene. LI. Fang *et al.* found a specific capacitance of 305.3 F/g for CNT/PANI composite with a 50 nm thick coating of PANI over CNT. Similarly, L. B. Kong *et al.* obtained the highest specific capacitance value of 224 F/g for the MWCNTs/PANI nanocomposite materials containing MWCNTs of 0.8 wt% [17]. In case of graphene based PANI composites A. V. Murugan reported highest specific capacitance of 408 F/g for (1:1) weight of PANI and graphene [18]. TiO_2 is a non-toxic, low cost transition metal oxide and available in abundance. Various composite materials for supercapacitor applications containing TiO_2 have been investigated in detail. Reddy *et al.* obtained a specific capacitance of 166 F/g for TiO_2/MWCNTs nanocrystalline composite by chemical reduction method [9]. C. Bian *et al.* studied the fibriform polyaniline/nano-TiO_2 composite containing 80% conducting polyaniline by mass which showed maximum specific capacitance of 330 F/g at a constant current density of 1.5 A/g [19]. Further, A. K. Mishra and S. Ramaphrabu found a maximum specific capacitance of 265 F/g for TiO_2 decorated functionalised graphene [20]. However in our present work, we have prepared three nanocomposites based on MWCNTs/PANI, TiO_2-MWCNTs/PANI and graphene/TiO_2-MWCNTs/PANI, where the composition of graphene: TiO_2-MWCNTs is 9:1 by weight. The samples have been prepared by in situ oxidative polymerisation method and their efficiency as supercapacitor electrode material has been studied extensively.

2. Experimental

2.1. Apparatus and Reagents

MWCNTs were obtained from Iljin Nano Technology, Korea, (95% purity and 20 - 40nm diameter). Graphene was obtained from Sinocarbon Materials Technology Co. Ltd. China. Ammonium persulphate (APS), Cetyltrimethylammoniumbromide (CTAB) were supplied by Loba-Chemie Pvt. Ltd. Mumbai (India). Aniline was obtained from E. Merck Ltd. (India). Titanium(IV) n-butoxide and iso-propanol were purchased from Sigma Aldrich. All the chemicals were used without any further purification.

2.2. Preparation of Nanocomposites

Titanium oxide (TiO_2) coated MWCNTs have been synthesised by following a sol-gel process, already reported by Siu-Ming Yuen *et al.* [21]. In brief, MWCNTs were dispersed in iso-propanol and it was followed by addition of Titanium(IV) n-butoxide and distilled water in a weight ratio of MWCNT:titanium(IV) n-butoxide:iso-propanol: water (1:0.3:50:25). The whole reaction mixture was kept at room temperature for 48 hours and then the isopropanol was evaporated by heat treatment to obtain TiO_2 coated MWCNTs. Nanocomposites based on unmodified MWCNTs/PANI and TiO_2 modified MWCNTs/PANI were prepared by insitu oxidative polymerisation of aniline, reported elsewhere. 60 mg MWCNTs were dispersed in water by using cetyltrimethyl ammonium bromide (CTAB) as dispersing agent by ultrasonication for 30 minutes using ultrasonic processor, Sonapros PR-250. To that suspension, 0.6 ml aniline monomer was added and sonicated for further 10 minutes. Subsequently, ammonium persulphate (APS) solution containing 2.04 gm APS was added and the sonication was continued for another 20 minutes. Then the whole suspension was kept at 0°C - 5°C for 12 hours, filtered and washed with water ethanol solution to remove the unreacted monomer and the residue was dried to get MWCNTs/PANI nanocomposites. The same procedure was followed for the TiO_2-MWCNTs/PANI and graphene/TiO_2-MWCNT/PANI composites preparation. For preparation of the graphene/TiO_2-MWCNTs/PANI nanocomposites, the weight ratio initially taken for the graphene to TiO_2-MWCNTs was (9:1).

2.3. Fabrication of Electrode

For fabrication of the electrode for electrochemical characterisations the nanocomposites were dispersed in 1% nafion solution via sonication. The nafion solution was prepared by mixing 10 µl nafion in 1ml dehydrated ethanol. The well dispersed samples were casted onto the glassy carbon (GC) electrode surface (diameter –3 mm) and completely dried in air. Here the GC electrode acted as working electrode.

3. Results and Discussion

3.1. Fourier Transform Infrared Spectroscopy (FTIR) Study

FTIR of the MWCNTs and graphene based nanocomposites was performed using a NEXUS 870 FTIR (Thermo Nicolet) to investigate the formation of PANI in presence of TiO_2 coated MWCNTs and TiO_2 coated CNT/graphene nanocomposites and the plot is shown in **Figure 1**. The peak at 1575 cm^{-1} indicates the C=C stretching frequency of the quinoid ring of the PANI unit, whereas the peak at 1464 cm^{-1} indicates the C=C stretching of the benzenoid ring [22] that shifts to 1485 cm^{-1} for the graphene/TiO_2-MWCNTs/PANI. The peaks at 1299 cm^{-1} and 801 cm^{-1} denote the C-N stretching and C-C or C-H stretching of benzenoid unit. The peak at 3433 cm^{-1} can be attributed to the N-H stretching frequency [23]. For the TiO_2 coated MWCNTs/graphene/PANI composite the peak gets broadened near 3435 cm^{-1} probably due to some moisture absorption thereby O-H stretching frequency contributing to some extent. The peaks at 2855 cm^{-1} and 2923 cm^{-1} are associated with the symmetric and asymmetric vibrations of C-H bond [23,24]. All these FTIR data indicate the formation of PANI for both the composites. The peak at 608 cm^{-1} indicates the Ti-O stretching frequency of the TiO_2 unit thus confirming the formation of TiO_2 over MWCNT [25].

3.2. XRD Analysis

The modification of MWCNTs surface by TiO_2 was confirmed by the XRD analysis using a Rigaku difractometer with a Cu Kα radiation (λ = 1.54056 cm^{-1}). **Figure 2** shows the XRD pattern of pure MWCNTs, TiO_2 coated MWCNTs and graphene/TiO_2-MWCNTs/PANI nanocomposite. For pure MWCNTs, the strong and sharp
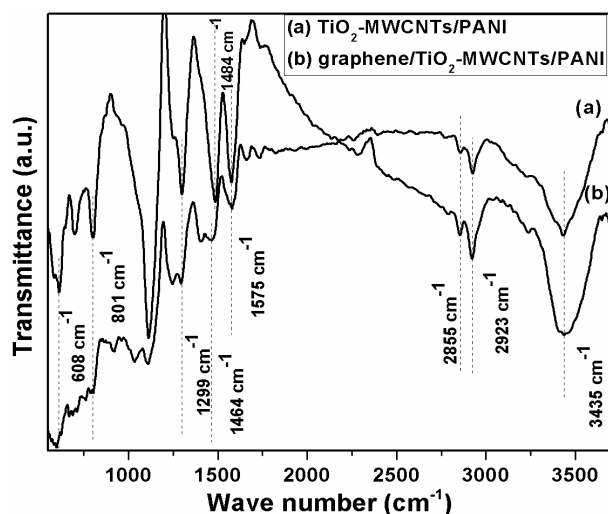
diffraction peak at 26° corresponds to (022) reflections of MWCNTs. In case of TiO_2 coated MWCNTs, additional peaks appear at scattering angles 25.36°, 37.95°, 48.12°, 53.98°, 55.12° and 62.75° corresponding to the reflections from (101), (004), (200), (105), (211), (204) crystalline plane respectively [26]. This indicates the crystalline nature of the TiO_2 coated MWCNTs. However in case of the composite, the corresponding peak at 25.24°, which is a characteristic peak of pure PANI is absent which means that most of the PANI is deposited on the surface of the TiO_2 coated MWCNTs [19]. This is an advantage as it shortens the diffusion path of the electrolyte and provides a larger electrochemical surface.

3.3. Morphological Characterizations

The surface morphologies of the as prepared nanocomposites were analysed by FESEM using Carl Zeiss-SU-PRATM 40 with an accelerating voltage of 5 kV. The samples were first gold coated to make the surface well conducting. **Figures 3(a)-(c)** represent the FESEM images of pristine MWCNTs, graphene and neat PANI. The FESEM image gives the evidence of smooth surface of the pristine MWCNTs and graphene. The FESEM images of the TiO_2-MWCNTs/PANI and graphene/TiO_2-MWCNTs/PANI nanocomposites are shown in **Figures 3(d)** and **(e)** which show a uniform coating of the PANI over the as prepared TiO_2 modified MWCNTs surface which makes the surface rough. For further analysis, transmission electron microscopy (TEM) was carried out by using TECNAI G2-20S-TWIN inorder to inspect the extent of dispersion of the in situ formed PANI in the nanocomposites. For the TEM analysis the samples were well dispersed in acetone and a drop was placed on a copper grid and dried in air. Samples subjected to both FESEM and TEM analyses were prepared at room tem-
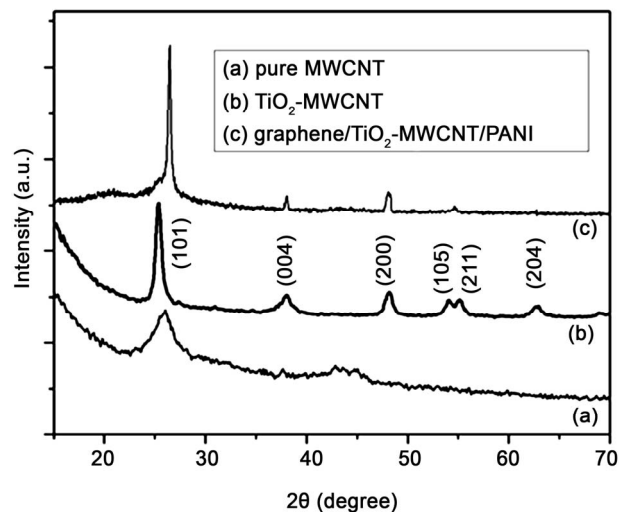

Figure 1. FTIR of TiO2-MWCNTs/PANI and graphene/TiO₂-MWCNTs/PANI.

Figure 2. XRD pattern of MWCNTS, TiO₂ coated MWCNTs and graphene/TiO₂-MWCNTs/PANI.

perature. **Figures 4(a)-(c)** represent the TEM images of neat MWCNTs, neat graphene and neat PANI. The TEM image of TiO_2 coated MWCNTs is shown in **Figure 4(d)**. The presence of TiO_2 makes the MWCNTs surface rough. **Figure 4(e)** represents the TEM image of graphene/TiO_2-MWCNTs/PANI. From the picture, it is clear that PANI is uniformly coated onto the TiO_2-MWCNTs and Graphene surface and forms a sandwiched structure in the nanocomposite.

3.4. Electrochemical Characterizations

Electrochemical characterisations such as Cyclic Voltammetry (CV) and Electrochemical Impedance Spectroscopy (EIS) of the prepared nanocomposites were carried out by GAMRY Ref 3000 instrument by using a three electrode system where platinum and saturated calomel electrode (SCE) were used as counter and reference electrodes respectively. For the electrochemical characterizations potential window was chosen from
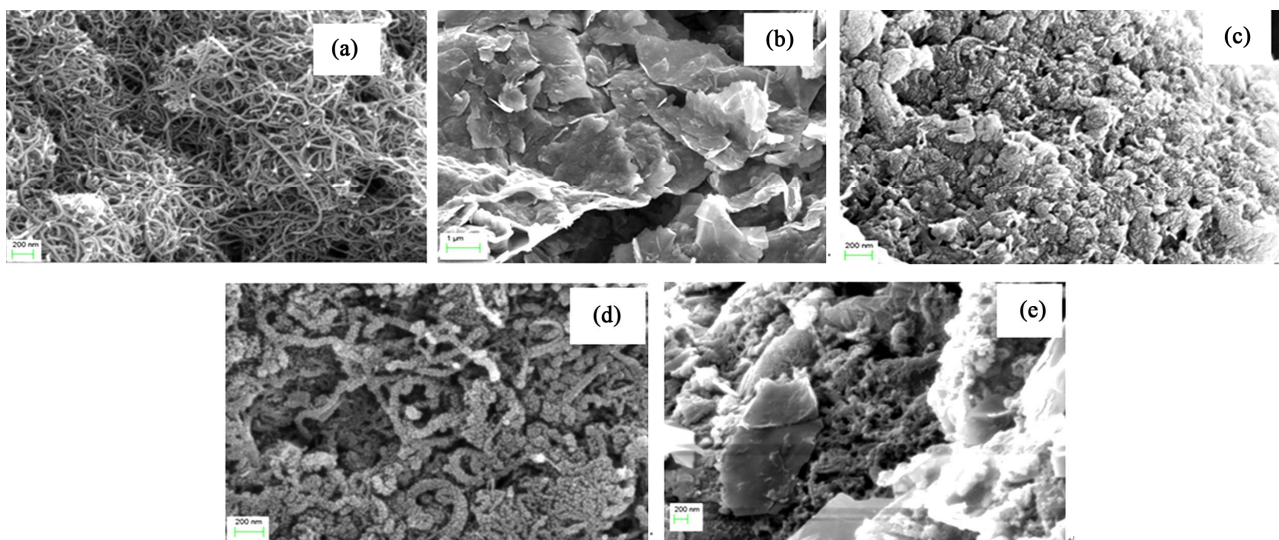

Figure 3. FESEM image of (a) neat MWCNTs; (b) Graphene; (c) Neat PANI; (d) TiO_2-MWCNTs/PANI and (e) Graphene/ TiO_2-MWCNTs/PANI.
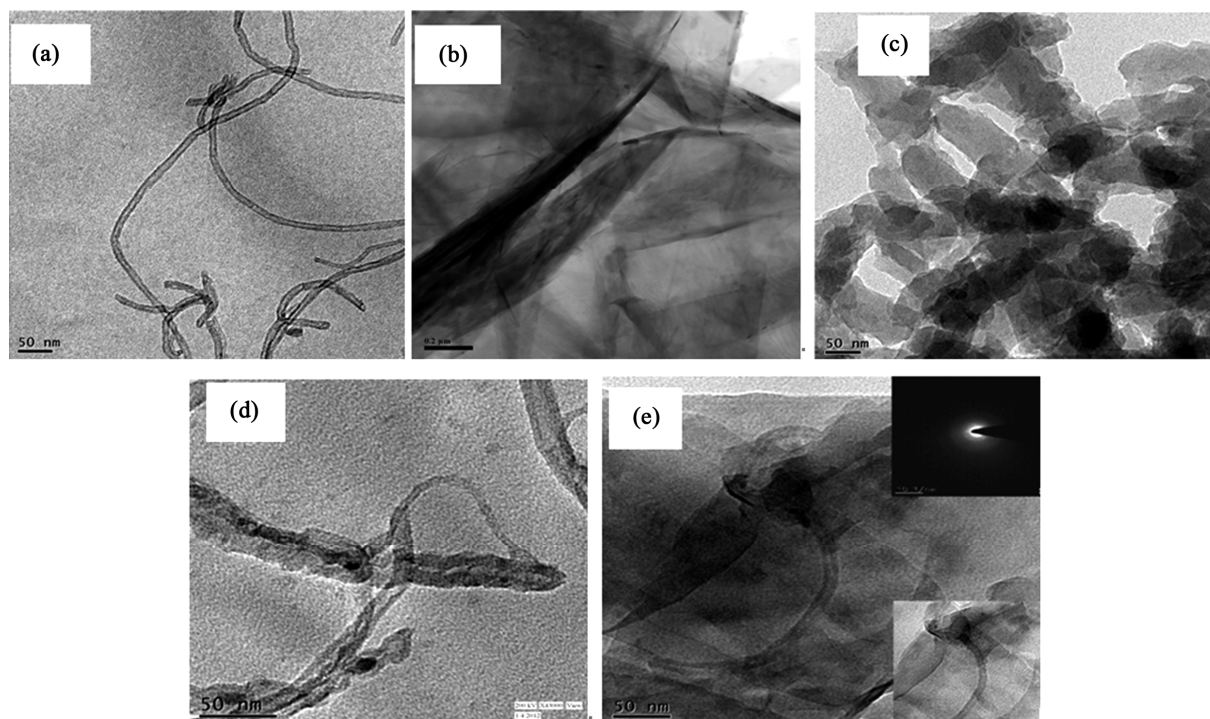

Figure 4. TEM image of (a) MWCNTs; (b) Graphene; (c) Pure PANI; (d) TiO_2 coated MWCNTs and (e) Graphene/ TiO_2-MWCNTs/PANI (SAED image is shown in inset).

(−0.7 V to +0.7 V) under which the nanocomposites showed excellent electrochemical behaviour and the electrolyte used was 1 M KCl. The specific capacitance (Cs in F/g) of the nanocomposites from the CV measurement are calculated by using the following equation [27].

$$\text{Specific capacitance: } C_s = \frac{\int_{V_1}^{V_2} I(V) \, dV}{(V_2 - V_1)vm} \qquad (1)$$

where, $I(V)$ is the instantaneous current in CV, $\int_{V_1}^{V_2} I(V) \, dV$ is the area under the I-V curve, v is the scan rate (V/s), $(V_2 - V_1)$ is the potential window and m is the mass of the electroactive material. **Figure 5(a)** represents the CV plots of MWCNTs/PANI, TiO$_2$-MWCNTs/PANI and graphene/TiO$_2$-MWCNTs/PANI composites at 10 mV/s scan rate which showed specific capacitance respectively, 114 F/g, 158.09 F/g, and 269.46 F/g. The highest specific capacitance value obtained for the TiO$_2$-MWCNTs/PANI composite was 443.57 F/g at 2 mV/s scan rate. Upon addition of graphene at a weight percentage of (9:1) to that of TiO$_2$ coated MWCNTs, the specific capacitance value increases tremendously. The highest specific capacitance obtained for the nanocomposite, graphene/TiO$_2$-MWCNTs/PANI was 666.3 F/g at 2 mV/s scan rate. For MWCNTs/PANI composite the combination of MWCNTs and PANI shows superior performance than the individual component (already reported) possibly due to the combination of easy electrolyte accessibility and a reduction in diffusion distance.

However, the better activity of the TiO$_2$-MWCNTs/PANI is due to the better synergism between the PANI and the TiO$_2$ modified MWCNTs surface. TiO$_2$ is an n-type semiconductor and the surface charge is more than the other region due to the effective contribution of the positively charged depletion region [28]. Incorporation of graphene causes an increase in the surface area on which PANI can grow. This improves the area of contact with the electrolyte and an improved conductivity in the redox pseudocapacitive composite structure results in an increased supercapacitance. The CV plot of graphene/TiO$_2$-MWCNTs/PANI at various scan rates are given in **Figure 5(b)**. The non-rectangular nature of the CV curve and presence of peaks at low scan rate indicate deviation from ideal behaviour and the considerable contribution of pseudocapacitance to the total specific capacitance. The pseudocapacitance can arise due to both TiO$_2$ and PANI. **Figure 5(c)** represents the variation of specific capacitance with scan rate for the two composites. The energy density and power density of the composites are calculated by using the following equations [29]

$$\text{Energy density} \qquad E = 1/2 C_s V^2 \qquad (2)$$

$$\text{Power density} \qquad P = E/T \qquad (3)$$

where C_s is the specific capacitance in F/g, V is the operating voltage range in Volt and T is the discharge time. The highest value of energy density for TiO$_2$-MWCNTs/PANI and graphene/TiO$_2$-MWCNTs/PANI was respectively 120.75 Wh/kg and 181.3 Wh/kg at 2 mV/s scan rate whereas highest power density was respectively 3152 W/kg and 5142.85 W/kg at 200 mV/s scan rate.
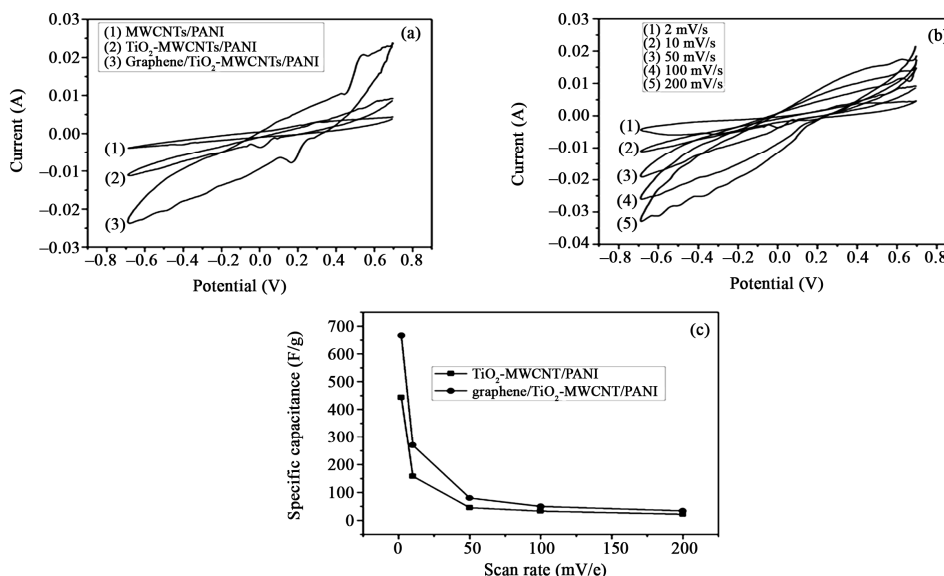

Figure 5. Comparison of CV plot of MWCNTs/PANI, TiO$_2$-MWCNTs/PANI and graphene/TiO$_2$-MWCNTs/PANI at 10 mV/s scan rate (a), CV plot of graphene/TiO$_2$-MWCNTs/PANI nanocomposites at 2 mV/s, 10 mV/s, 50 mV/s, 100 mV/s and 200 mV/s scan rate (b), and Variation of specific capacitance of TiO$_2$-MWCNTs/PANI and graphene/TiO$_2$-MWCNTs/PANI with scan rate (c).

Various values of specific capacitance, energy density and power density obtained at different scan rates are given in **Tables 1** and **2**.

3.5. Electrochemical Impedance Spectroscopy

Electrochemical Impedance Spectroscopy (EIS) was carried out by using GAMRY ref.3000 using an ac voltage amplitude 5 mV between the frequency range 0.1 Hz to 1 MHz. EIS is a very important and useful technique to formulate a hypothesis when the EIS experimental data is fitted with an suitable equivalent circuit model. Thus it is a convenient tool to obtain many a electrochemical information such as, electrolyte resistance, charge transfer resistance, double layer capacitance etc. [30]. The Nyquist plots of the nanocomposites for analysis the EIS data are shown in **Figure 6(a)**. The equivalent circuit to which the EIS data was fitted is shown in **Figure 6(b)**. For an ideal capacitor the impedance plot should be a vertical line and parallel to the imaginary impedance axis. However our as prepared nanocomposites show deviation from ideality. The non-ideal behaviour of the nano-composites may be due to the constant phase element (CPE) which arises due to (1) rough surface of the electrode, (2) different thickness of coating, (3) non-uniform distribution of current due to edge effect and (4) distribution of reaction rate at surface due to distribution of active sites with different activation energies. CPE corresponds to the capacitance and follow the equation, $Z_{CPE} = Z(jw)^{-n}$, where n is the CPE constant and ranges from zero to one. Generally for supercapacitor, n varies from 0.5 to 1. n = 0 indicates the resistor, n = 1 indicates the ideal capacitor and n = 0.5 indicates the Warburg behaviour. It can be seen that all the nanocomposites show a semicircle loop at higher frequency region indicating charge transfer resistance. In the lower frequency region the imaginary part of the impedance sharply increases indicating capacitive behaviour of the nanocomposites. The graphene/TiO_2-MWCNTs/PANI nanocomposite shows much higher impedance in the lower frequency region compared to that of other two nanocomposites. The information obtained from the EIS after fitting it to an equivalent circuit model is shown in **Table 3**.

Table 1. Various values of specific capacitance (F/g), energy density (Wh/kg) and Power density (W/kg) obtained for TiO$_2$-MWCNTs/PANI nanocomposites at different scan rate.

Scan rate	2 mV/s	10 mV/s	50 mV/s	100 mV/s	200 mV/s
Specific capacitance	443.57	158	45.59	33.82	22.5
Energy density	120.75	43.03	12.41	9.2	6.2
Power density	621	1106.53	1595	2365.7	3152

Table 2. Various values of specific capacitance (F/g), energy density (Wh/kg) and power density (W/kg) obtained for graphene/TiO$_2$-MWCNTs/PANI nanocomposites at different scan rate.

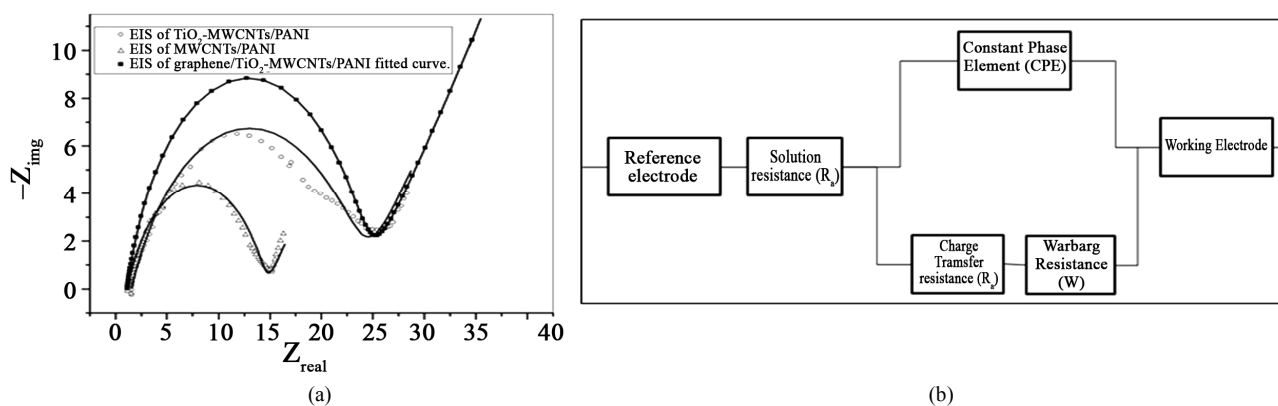| Scan rate	2 mV/s	10 mV/s	50 mV/s	100 mV/s	200 mV/s
Specific capacitance	666.3	269.464	80.27	50	33.89
Energy density	181.3	73.35	21.85	14	10
Power density	932	1866	2809.4	3600	5142.85

(a)   (b)

Figure 6. EIS plot of MWCNTs/PANI, TiO$_2$-MWCNTs/PANI and graphene/TiO$_2$-MWCNTs/PANI (a), equivalent circuit model to which the EIS data are fitted (b).

Table 3. Fitting data for equivalent electrical circuit elements of MWCNTs/PANI, TiO$_2$-MWCNTs/PANI and graphene/ TiO$_2$-MWCNTs/PANI nanocomposites.

	Solution resistance (R$_s$) ohms)	CPE, Y$_0$, (S × s^n)	Freq. power (0 < n ≤ 1)	Chargen transfer resistance(R$_{ct}$) (ohms)	Warburg (W) resistance (S × s$^{1/2}$) (ohms)
MWCNT/PANI	1.538	456.6e^{-6}	0.681	24.60	185.5e^{-3}
TiO2-MWCNT/PANI	1.159	248.1e^{-6}	0.729	13.47	486.9e^{-3}
graphene/ TiO2-MWCNT/PANI	1.123	78.12e^{-6}	0.857	23.64	79.13e^{-3}

4. Conclusion

In this study, the TiO$_2$-MWCNTs/PANI and graphene/ TiO$_2$-MWCNTs/PANI nanocomposites were successfully prepared by in situ oxidative polymerisation method. The two nanocomposites showed maximum specific capacitances of 443.57 F/g and 666.3 F/g respectively at 2 mV/s scan rate in 1M KCl. The TiO$_2$-MWCNTs acted as current collector as well as conducting wire interconnected among the graphene and PANI. The graphene/ TiO$_2$-MWCNTs/PANI composite showed high energy density of 181.3 Wh/kg and very high power density of 5142.85 W/kg which were higher than that of TiO$_2$-MWCNTs/PANI. The reasonably high value of energy density and power density ensure the nanocomposite functions as an efficient supercapacitor electrode material.

REFERENCES

[1] B. E. Conway, "Electrochemical Supercapacitors: Scientific Fundamentals and Technological Applications," Kluwer Academic/Plenum, New York, 1999

[2] P. Simon and Y. Gogotsi, "Materials for Electrochemical Capacitors," *Nature Materials*, Vol. 7, No. 11, 2008, pp. 845-854. doi:10.1038/nmat2297

[3] S. Sarangpani, B. V. Tilak and C. P. Chen, "Materials for Electrochemical Capacitors," *Journal of the Electrochemical Society*, Vol. 143, No. 11, 1996, pp. 3791-3799. doi:10.1149/1.1837291

[4] K. H. An, K. K. Jeon, J. K. Heo, S. C. Lim, D. J. Bae and Y. H. Lee, "High-Capacitance Supercapacitor Using a Nanocomposite Electrode of Single-Walled Carbon Nanotube and Polypyrrole," *The Electrochemical Society*, Vol. 149, No. 6, 2002, pp. A1058-A1062. doi:10.1149/1.1491235

[5] Z. A. Hu, Y. L. Xie, Y. X. Wang, L. P. Mo, Y. Y. Yang, and Z. Y. Zhang, "Polyaniline/SnO$_2$ Nanocomposite for Supercapacitor Applications," *Materials Chemistry and Physics*, Vol. 114, No. 2-3, 2009, pp. 990-995. doi:10.1016/j.matchemphys.2008.11.005

[6] R. N. Reddy and R. G. Reddy, "Sol-Gel MnO$_2$ as an Electrode Material for Electrochemical Capacitors," *Journal of Power Sources*, Vol. 124, No. 1, 2003, pp. 330-337. doi:10.1016/S0378-7753(03)00600-1

[7] W. Sugimoto, K. Tizaki, K. Yokoshima, Y. Murakami and Y. Takasu, "Evaluation of the Pseudocapacitance in RuO$_2$ with a RuO$_2$/GC thin Film Electrode," *Electrochimica Acta*, Vol. 49, No. 2, 2004, pp. 313-320. doi:10.1016/j.electacta.2003.08.013

[8] F. B. Zhang, Y. K.Zhou and H. L. Li, "Nanocrystalline NiO as an Electrode Material for Electrochemical Capacitor," *Materials Chemistry and Physics*, Vol. 83, No. 2-3, 2004, pp. 260-264. doi:10.1016/j.matchemphys.2003.09.046

[9] A. L. M. Reddy and S. Ramaprabhu, "Nanocrystalline Metal Oxides Dispersed Multiwalled Carbon Nanotubes as Supercapacitor Electrodes," *Journal of Physical Chemistry C*, Vol. 111, No. 21, 2007, pp. 7727-7734. doi:10.1021/jp069006m

[10] Q. Cheng, J. Tang, J. Ma, H. Zhang, N. Shinya and L. C. Qin, "Graphene and Nanostructured MnO$_2$ Composite Electrodes for Supercapacitors," *Carbon*, Vol. 49, No. 9, 2011, pp. 2917-2925. doi:10.1016/j.carbon.2011.02.068

[11] H. Wang, Y. Liang, T. Mirfakhrai, Z. Chen, H. S. Casalongue and H. Dai, "Advanced Asymmetrical Supercapacitors Based on Graphene Hybrid Materials," *Nano Research*, Vol. 4, No. 8, 2011, pp. 729-736. doi:10.1007/s12274-011-0129-6

[12] A. Burke, "Ultracapacitors: Why, How, and Where Is the Technology," *Journal of Power Sources*, Vol. 91, No. 1, 2000, pp. 37-50. doi:10.1016/S0378-7753(00)00485-7

[13] J. Chmiola, G. Yushin,Y. Gogotsi, C. Portet, P. Simon and P. L. Taberna, "Anomalous Increase in Carbon Capacitance at Pore Sizes Less than 1 Nanometer," *Science*, Vol. 313 No. 5794, 2006, pp. 1760-1763. doi:10.1126/science.1132195

[14] H. L. Wang, Q. L. Hao, X. J. Yang, L. D. Lu and X. Wang, "Graphene Oxide Doped Polyaniline for Supercapacitors," *Electrochemistry Communications*, Vol. 11, No. 6, 2009, pp. 1158-1161. doi:10.1016/j.elecom.2009.03.036

[15] G. Lota, T. A. Centeno, E. Frackowiak and F. Stoeckli, "Improvement of the Structural and Chemical Properties of a Commercial Activated Carbon for Its Application in Electrochemical Capacitors," *Electrochimica Acta*, Vol. 53, No. 5, 2008, pp. 2210-2216. doi:10.1016/j.electacta.2007.09.028

[16] J. D. Madden, A. I. Najafabadi and D. T. H. Tan, "Towards High Power Polypyrrole/Carbon Capacitors," *Synthetic Metals*, Vol. 152, No. 1-3, 2005, pp. 129-132. doi:10.1016/j.synthmet.2005.07.094

[17] L. B. Kong, J. Zhang, J. J. An, Y. C. Luo and L. Kang, "MWNTs/PANI composite Materials Prepared by *In-Situ* Chemical Oxidative Polymerization for Supercapacitor

Electrode," *Journal of Materials Science*, Vol. 43, No. 10, 2008, pp. 3664-3669. doi:10.1007/s10853-008-2586-1

[18] A. V. Murugan, T. Muraliganth and A. Manthiram, "Rapid, Facile Microwave-Solvothermal Synthesis of Graphene Nanosheets and Their Polyaniline Nanocomposites for Energy Strorage," *Chemistry of Materials*, Vol. 21, No. 21, 2009, pp. 5004-5006. doi:10.1021/cm902413c

[19] C. Bian, A. Yu and H. Wu, "Fibriformpolyaniline/Nano-TiO$_2$ Composite as an Electrode Material for Aqueous Redox Supercapacitors," *Electrochemistry Communications*, Vol. 11, No. 2, 2009, pp. 266-269. doi:10.1016/j.elecom.2008.11.026

[20] A. K. Mishra and S. Ramaphrabu, "Functionalized Graphene-Based Nanocomposites for Supercapacitor Application," *The Journal of Physical Chemistry C*, Vol. 115, No. 29, 2011, pp. 14006-14013. doi:10.1021/jp201673e

[21] S. M. Yuen, C. C. M. Ma, C. Y. Chuang, Y. H. Hsiao, C. L. Chiang and A. D. Yu, "Preparation, Morphology, Mechanical and Electrical Properties of TiO$_2$ Coated Multi-walled Carbon Nanotube/Epoxy Composites," *Composites*: *Part A*, Vol. 39, No. 1, 2008, pp. 119-125. doi:10.1016/j.compositesa.2007.08.021

[22] S. K. Pillalamarri, F. D. Blum, A.T. Tokuhiro, J. G. Story, and M. F. Bertino, "Radiolytic Synthesis of Polyaniline Nanofibers: A New Templateless Pathway," *Chemistry of Materials*, Vol. 17, No. 2, 2005, pp. 227-229. doi:10.1021/cm0488478

[23] T. C. Girija and M. V. Sangaranarayanan, "Polyaniline-Based Nickel Electrodes for Electrochemical Supercapacitors—Influence of Triton X-100," *Journal of Power Sources*, Vol. 159, No. 2, 2006, pp. 1519-1526. doi:10.1016/j.jpowsour.2005.11.078

[24] Y. Qiao, C. M. Li, S. J. Bao and Q. L. Bao, "Carbon Nanotube/Polyaniline Composite as Anode Material for Microbial Fuel Cells," *Journal of Power Sources*, Vol. 170, No. 1, pp. 79-84. doi:10.1016/j.jpowsour.2007.03.048

[25] P. M. Kumar, S. Badrinarayanan and M. Sastry, "Nanocrystalline TiO$_2$ Studied by Optical, FTIR and X-Ray Photoelectron Spectroscopy: Correlation to Presence of Surface States," *Thin Solid Films*, Vol. 358, No. 1-2, 2000, pp. 122-130. doi:10.1016/S0040-6090(99)00722-1

[26] Y. Zhao, Y. Hu, Y. Li, H. Zhang, S. Zhang, L. Qu, G. Shi and L. Dai "Super-Long Aligned TiO$_2$/Carbon Nanotube Arrays," *Nanotechnology*, Vol. 21, No. 50, 2010, p. 505702. doi:10.1088/0957-4484/21/50/505702

[27] Z. Fan, M. Xie, Xi Jin, J. Yan and T. Wei, "Characteristics and Electrochemical Performances of Supercapacitors Using Double-Walled Carbon Nanotube/δ-MnO$_2$ Hybrid Material Electrodes," *Journal of Electroanalytical Chemistry*, Vol. 659, No. 2, 2011, pp. 191-195. doi:10.1016/j.jelechem.2011.05.025

[28] F. Fabregat-Santiago, I. Mora-Seró, G. Garcia-Belmonte and J. Bisquert, "Cyclic Voltammetry Studies of Nanoporous Semiconductors. Capacitive and Reactive Properties of Nanocrystalline TiO$_2$ Electrodes in Aqueous Electrolyte," *The Journal of Physical Chemistry B*, Vol. 107, No. 3, 2003, pp. 758-768. doi:10.1021/jp0265182

[29] J. Yan, T. Wei, B. Shao, Z. Fan, W. Qian, M. Zhang and F. Wei, "Preparation of a Graphene Nanosheet/Polyaniline Composite with High Specific Capacitance," *Carbon*, Vol. 48, No. 2, 2010, pp. 487-493. doi:10.1016/j.carbon.2009.09.066

[30] M. Ates and A. S. Sarac, "Electrochemical Impedance Spectroscopic Study of Polythiophenes on Carbon Materials," *Polymer Plastics Technology and Engineering*, Vol. 50, No. 11, 2011, pp. 1130-1148. doi:10.1080/03602559.2011.56630